Journal of Multidisciplinary Engineering Science and Technology (JMEST)
ISSN: 2458-9403
Vol. 3 Issue 5, May - 2016

Heat Generation and Transfer of Linear Rolling Guides Under Starved Lubrication

Haitian Zou[1, a], Baolin Wang[2, b], Feifei Wang[3, c]

[1] Graduate School at Shenzhen, Harbin Institute of Technology, Harbin 150001, P.R. China

[2] Institute for Infrastructure Engineering Western Sydney University, Locked Bag 1797, Penrith, NSW 2751, Australia

[3] College of Mechanical Engineering, Inner Mongolia University for the Nationalities, Tongliao, Inner Mongolia 028000, P.R. China

[a] zouhaitian945@gmail.com, [b] b.wang@uws.edu.au, [c] wff8610210@163.com

***Abstract*—Friction heat generated in the linear guide will degrade its transmission precision and greatly affects the motion accuracy of a high-precision mechanical system. This paper investigates the thermal behavior of a lubricant-starved linear rolling guide during operation. The equivalent heat flux generated at the contact interface of the linear guide was calculated by considering sliding friction, spinning friction and elastic hysteresis friction. A finite element (FE) model was established, and the temperature field of the linear guide was obtained by heat transfer analysis. As a validation of the numerical model with analytical heat flux and convection parameters, we setup a simple linear guide system to obtain the temperature at the specified monitoring points with NI measuring system. The numerical results agree well with the experimental data, which indicates that the proposed FE model and analytical method can accurately quantify the heat generation and transfer processes of the linear rolling guides during operation. This paper is useful for predicting the thermal behavior of the linear guides and also can be seen as a foundation for the thermal dynamics analysis of a wide range of ball bearings.**

Keywords—friction heat; numerical model; linear rolling guides

I. INTRODUCTION

Thermally induced err can account for as much as 70% of the total machining err of a high-precision machine tool [1,2], which greatly degrade the dynamic performance of the system. The frictional heat generated from joints is one of the principal heat sources of the internal heat of the system. In practical engineering, ball screw and linear rolling guide are the most commonly used joints in modern machine tools. However, previous studies mainly focused on the thermal behavior of the former, although they have the same contact characteristics [3-12]. By contrast, little research on liner rolling guides has been discussed due to their low heat generation. In fact, when the linear rolling guide system under starved lubrication and abnormal operating conditions, the thermal effect will be significant and cannot be ignored.

The complexity of the structure increases the difficulty of quantifying the heat transfer process of the linear rolling guide during operation by an analytical method. In fact, it is also impractical to establish a real semi-closed structure of the linear rolling guide with recirculating balls to model the heat generation and heat transfer process, because the poor and mismatch mesh, complicated contact condition and convergence problem will greatly degrade the precision of the numerical simulation, and make the results unreliable [13,14]. This paper investigates the heat generation and heat transfer process of the linear rolling guides by an analytical method combined with finite element (FE) thermal analysis. The heat flux generated at the contact rolling interface of the linear guide was calculated by considering sliding friction, spinning friction and elastic hysteresis friction, and then the FE model was established to obtain the temperature field of the whole structure by heat transfer analysis with the analytical heat flux. Finally, we established a simple linear guide system, and the temperature tests were performed to validate the FE model and the calculated thermal parameters.

II. THERMAL MODELING

We established a FE thermal model to obtain the steady state temperature of the linear rolling guide during operation. Here, the friction heat generated at the contact interface between the ball and raceway was replaced by heat flux directed to the contact surface of elliptical region. In addition, the convection effect of the whole structure was also considered in the numerical model.

A. Frictions and Heat Source Indensity

There exist three major types of friction at the ball-raceway contact of the linear rolling guides during operation: Sliding friction, Elastic hysteresis friction and Spinning friction. They are described below.

Fig. 1 shows the geometry of the contact ellipse of ball-raceway contact and sliding directions in contact zones. It can be seen that there exist two opposite sliding motions within the contact ellipse. The sliding friction f_c in the contact between ball and raceway is

$$f_\lambda = \int_{\mathrm{I}} \mu_\lambda p(x,y)\, ds - \int_{\mathrm{II}} \mu_\lambda p(x,y)\, ds \qquad (1)$$

where μ_λ is the friction coefficient, p is the contact pressure inside the elliptical region, and can be described as

$$p_{ij}(x,y)=\frac{3P_{ij}}{2\pi a_{ij}b_{ij}}\left[1-\left(x/a_{ij}\right)^2-\left(y/b_{ij}\right)^2\right]^{\frac{1}{2}} \quad (2)$$

where suffixes *i* and *j* are the raceway number and ball number, and a_{ij}, b_{ij} are the semi-major axis and semi-minor axis of the contact ellipse of the *j*th ball-raceway contact in the *i*th raceway, respectively.

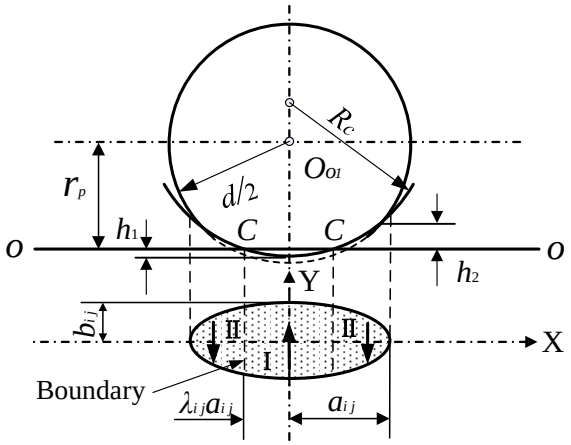

Fig. 1. *Geometry of contact ellipse and sliding directions in contact zones.*

Substituting (2) into (1), the $f_{\lambda ij}$ of the *j*th ball in the *i*th raceway can be calculated as:

$$f_{\lambda ij}=\mu_\lambda P_{ij}\left(\lambda_{ij}^3-3\lambda_{ij}+1\right) \quad (3)$$

where λ_{ij} is position parameter, which represents the position of the *j*th ball in pure rolling in the *i*th raceway, as shown in Fig. 1, and it can be calculated as follows.

Without loss of generality, the raceway number *i* and ball number *j* in the following equations are not represented to simply the calculation. Assuming the linear guide is in motion with constant velocity, the angular acceleration of the ball is zero. We have

$$I\frac{dw}{dt}=\int_{\mathrm{I}}\mu_\lambda p(x,y)\left(r_p+h_1\right)ds-\int_{\mathrm{II}}\mu_\lambda p(x,y)\left(r_p-h_2\right)ds=0 \quad (4)$$

where r_p is the vertical distance from the ball center O_{o1} to the transient rotation axis X-X, h_1 and h_2 are the distance from the point in contact zone I and the point in zone II to the rotation axis X-X, respectively. According to Fig. 1, they can be expressed as

$$\begin{cases} r_p=\dfrac{1}{2}\sqrt{d^2-4a^2}+\sqrt{R_c^2-a^2\lambda^2}-\sqrt{R_c^2-a^2} \\ h_1=\sqrt{R_c^2-x^2}-\sqrt{R_c^2-a^2\lambda^2}\ ,\ \left(-\lambda a<x<\lambda a\right) \\ h_2=\sqrt{R_c^2-a^2\lambda^2}-\sqrt{R_c^2-x^2}\ ,\ \left(\lambda a<|x|<a\right) \end{cases} \quad (5)$$

According to (4), we have

$$\left(\int_{\mathrm{I}}\mu_\lambda p(x,y)ds-\int_{\mathrm{II}}\mu_\lambda p(x,y)ds\right)r_p=\int_{\mathrm{I}}\mu_\lambda p(x,y)h_1ds+\int_{\mathrm{II}}\mu_\lambda p(x,y)h_2ds \quad (6)$$

Substituting (5) into the right side of (6), we can obtain

$$\int_{\mathrm{I}}\mu_\lambda p(x,y)h_1ds+\int_{\mathrm{II}}\mu_\lambda p(x,y)h_2ds=\mu_\lambda P\left(R_1-R_2-R_3\right) \quad (7)$$

Where

$$\begin{cases} R_1=\left(R_c^2-a^2\lambda^2\right)^{\frac{1}{2}}\left(\dfrac{1}{4}\lambda^3+\dfrac{3\lambda R_c^2}{8a^2}-\dfrac{3}{2}\lambda+1\right) \\ R_2=\left(R_c^2-a^2\right)^{\frac{1}{2}}\left(\dfrac{3R_c^2}{16a^2}+\dfrac{3}{8}\right) \\ R_3=\left(\dfrac{3R_c^4}{16a^3}-\dfrac{3R_c^2}{4a}\right)\left(2\arcsin\dfrac{\lambda a}{R_c}-\arcsin\dfrac{a}{R_c}\right) \end{cases} \quad (8)$$

According to (1), (3), (6) and (7), we have

$$\left(\lambda^3-3\lambda+1\right)r_p=R_1-R_2-R_3 \quad (9)$$

Assuming $R_c\approx d/2$, and letting $R_c/a\equiv D$. Substituting (5) and (8) into (9)

$$\left(-28\lambda^3+6\lambda D^2+72\lambda-16\right)\left(1-\frac{\lambda^2}{D^2}\right)^{\frac{1}{2}}=\left(3D^2+6\right)\left(1-\frac{1}{D^2}\right)^{\frac{1}{2}}+\left(3D^3-12D\right)\left(\arcsin\frac{1}{D}-\frac{1}{2}\arcsin\frac{\lambda}{D}\right) \quad (10)$$

Using the Taylor formula

$$\begin{cases} \left(1-\dfrac{\lambda^2}{D^2}\right)^{\frac{1}{2}}=1-\dfrac{1}{2}\left(\dfrac{\lambda}{D}\right)^2-\dfrac{1}{8}\left(\dfrac{\lambda}{D}\right)^4-\dfrac{1}{16}\left(\dfrac{\lambda}{D}\right)^6-\cdots \\ \left(1-\dfrac{1}{D^2}\right)^{\frac{1}{2}}=1-\dfrac{1}{2}\left(\dfrac{1}{D}\right)^2-\dfrac{1}{8}\left(\dfrac{1}{D}\right)^4-\dfrac{1}{16}-\cdots \\ \arcsin\dfrac{\lambda}{D}=\dfrac{\lambda}{D}+\dfrac{1}{6}\left(\dfrac{\lambda}{D}\right)^3+\dfrac{3}{40}\left(\dfrac{\lambda}{D}\right)^5-\dfrac{5}{112}\left(\dfrac{\lambda}{D}\right)^7+\cdots \\ \arcsin\dfrac{1}{D}=\dfrac{1}{D}+\dfrac{1}{6}\left(\dfrac{1}{D}\right)^3+\dfrac{3}{40}\left(\dfrac{1}{D}\right)^5-\dfrac{5}{112}\left(\dfrac{1}{D}\right)^7+\cdots \end{cases} \quad (11)$$

Neglecting the high order terms of (11), (10) can be rewritten as

$$6\lambda^5-\left(16D^2+8\right)\lambda^3+48\lambda D^2-16D^2+1=0 \quad (12)$$

Equation (12) is solved by a Matlab script, and the numerical results of λ is shown in the following Fig. 2.

It can be seen that the value of λ tends to reach a constant value of 0.347 with the increasing of *D* (0< *D* <20). For the linear rolling guide, *D* and λ are a_i dependent ($R_c/a_i\equiv A_i$). In general, 0.347 can be used for the friction calculation in (3).

The equivalent friction due to elastic hysteresis of the rolling ball is induced by the loss of the intermolecular friction energy, and it can be obtained by calculating the difference between the work done by the rolling moment (P_{ij} related) and the work done by the elastic restoring torque due to the material deformation [15]

$$f_{eij}=\frac{3\varepsilon_f P_{ij}^{\frac{4}{3}}}{8d_0}\left[\frac{3E\left(e,\frac{\pi}{2}\right)\sqrt{1-e_{ij}^{\,2}}}{\pi\sum\rho_{b-c}}\left(\frac{\left(1-\nu_b^{\,2}\right)}{E_b}+\frac{\left(1-\nu_c^{\,2}\right)}{E_c}\right)\right]^{\frac{1}{3}} \quad (13)$$

where ε_f is elasticity loss coefficient, d_0 is the ball diameter, $E\left(e,\pi/2\right)$ are the complete elliptic integrals of the second kind, $\sum\rho_{b-c}$ is the curvature sum of the carriage $\sum\rho_{b-c}=4/d_0-1/R_c$, R_c is the raceway groove radius of the carriage, E_b, ν_b, E_c and ν_c are the Young's modulus and Poisson's ratio of the ball and carriage.

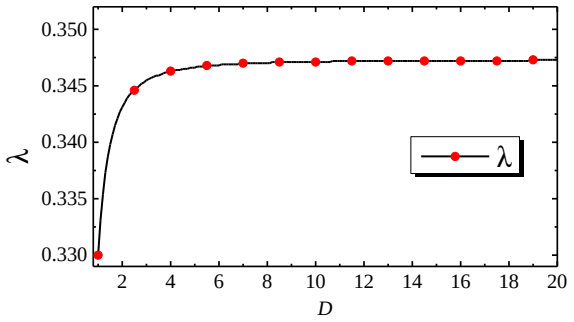

Fig. 2. *The value of λ with respect to constant D.*

The ball of bearings rolling in a raceway with nonzero contact angles will rotate about the normal of the contact surface, and the spinning force generated during the spinning contact motion can be calculated as [16]

$$f_{sij}=\frac{3\mu_s P_{ij}}{4d_0}\left[\frac{3P_{ij}\left[E\left(e,\pi/2\right)\right]^4}{4\pi\left(1-e_{ij}^{\,2}\right)\sum\rho_{b-c}}\left(\frac{4\left(1-\nu_b^{\,2}\right)}{E_b}+\frac{4\left(1-\nu_c^{\,2}\right)}{E_c}\right)\right]^{\frac{1}{3}} \quad (14)$$

where μ_s is the friction coefficient, e_{ij} is the eccentricity of the contact ellipse of the *j*th ball-raceway contact in the *i*th raceway.

The heat generated at the contact rolling interface can be obtained by the calculation of the work done by the three frictions as mentioned above. It is assumed that the total work is converted to heat, and it is divided equally between the ball and raceway. Then, the equivalent heat flux at the contact surface of the *i*th raceway can be calculated as

$$q_i=\frac{1}{2}\sum_{j=1}^{N}\frac{f_{ij}v}{a_{ij}L},\quad i=1,2,3,4 \quad (15)$$

where f_{ij} is the sum of three frictions, N is the number of the loaded balls in a raceway, v is the velocity of the linear guide, L is the length of the loading zone of balls.

B. Convection Parameter

The major heat loss of the linear rolling guide during operation is on its surfaces exposed to air. The convection parameter h is defined as $h=N_u k/L_S$, where k is the heat conductivity of air, L_S is the scaling length of the flow surface, N_u is the Nusselt number. For the surfaces of the carriage parallel to the air flow, N_u can be calculated as [17]

$$N_u=0.332P_r^{1/3}R_e^{1/2} \quad (16)$$

where P_r and R_e are Prandtl number and Reynolds number. For the surfaces of the carriage perpendicular to the air flow, N_u can be calculated as [18]

$$N_u=0.228P_r^{1/3}R_e^{0.731} \quad (17)$$

C. Boundary Conditions and Numerical Results

In practical engineering, the linear rolling guide will reach a thermal equilibrium after running a certain distance. The frictional heat generated at the contact rolling interface of the linear guide was obtained by (3), (13)-(15). Then the steady state heat transfer analysis was performed to obtain the temperature field of the system with the calculated heat flux. Here, the average velocity of the linear guide was 1.2/m/s, and the sink temperature was 25℃. When the vertical load F=0, P_i for *i*=1 and *i*=4 were calculated as P_1=156N, P_4=147N, and the heat flux q_i at the surface of the elliptical region of the *i*th raceway for *i*=1, 4 were calculated as $q_1=2.86\times10^3$w/m^2 and $q_4=2.72\times10^3$w/m^2, respectively. According to (16), (17), the convection coefficient of the top (side) surfaces of the carriage was calculated as 8.28 W/m^2/°C, and the front surface was 21.6 W/m^2/°C. In addition, heat radiation was ignored in the numerical model due to the relatively low surface temperature of the structure.

Fig. 3. shows the steady temperature field of linear rolling guide during operation. It can be seen that the contact elliptical region shows high temperature gradient. The peak temperature of the carriage is 32.1℃, and the maximum temperature rise is about 7℃. In addition, the local temperature of the upper raceway is similar with lower raceway, which can be ascribed to the similar reaction force generating similar frictional heat.

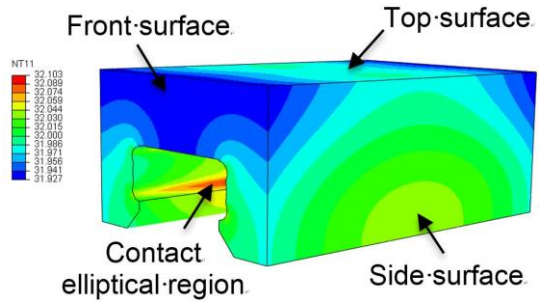

Fig. 3. *Temperature field of the linear rolling guide.*

III. EXPERIMENTAL SETUP

In order to verify the FEM thermal model and the analytical heat flux q_i used in this work, the surface temperature of the carriage under the same operating conditions with FEM analysis (no vertical load) was measured with the NI test system, as shown in Fig. 4. The measurement data were acquired by NI PXI-4351 module installed in a PXI-1033 signal acquisition system. The pt100 thermal sensors were attached to the surfaces of the carriage, which has a measuring resolution of 0.001℃. The tests were divided into two groups with the velocity of the carriage of 1.2m/s (Set 1) and 2.5m/s (Set 2) to quantify the temperature variations of the linear guide under different operating conditions. The environmental temperature is 25℃, and each test was continued until the steady state condition was attained.

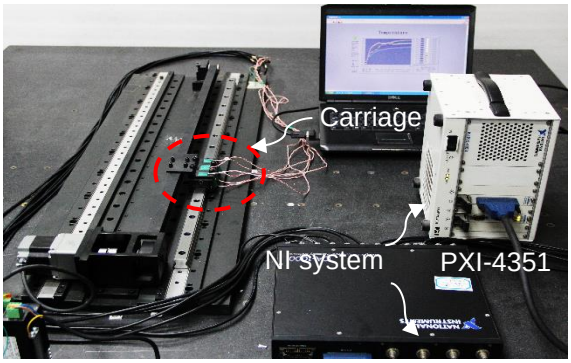

Fig. 4. *The measurement of temperature and pt100 thermal sensors.*

IV. RESULTS AND DISCUSSION

Fig. 5 and Fig. 6 show the locations of the thermal sensors and the measured temperatures of the carriage with a velocity of 1.2m/s. The experimental data show that all the surface temperatures of the carriage reach thermal equilibrium about half an hour. For the convenience of comparison, the numerical predicted and measured equilibrium temperatures of the carriage with velocities of 1.2m/s and 2.5m/s at the specified four monitoring locations are summarized in table I. It can be seen that when the environmental temperature is 25℃, the average temperature rise of the whole structure of set 1 and set 2 obtained by these two methods are (6.98, 7.88)℃ and (10.76, 11.85)℃, respectively. Both of these results also show that the temperature of the lateral side of the carriage is higher than that of the top side. In addition, the measured temperatures of the carriage are a little higher than the FEM calculated, this may be because the viscosity-related heat and frictional heat in non-load zone is ignored in the calculation of heat flux. On the whole, the FEM calculated temperatures of the carriage show good agreements with the experimental data, the percentage errs between the two methods results of the two sets data are no more than 3.24% and 3.17%, which indicates that the calculated heat flux and convection parameters are reliable, and the presented analytical method and FEM thermal model can accurately predict the heat generation and transfer processes of the linear rolling guide during operation.

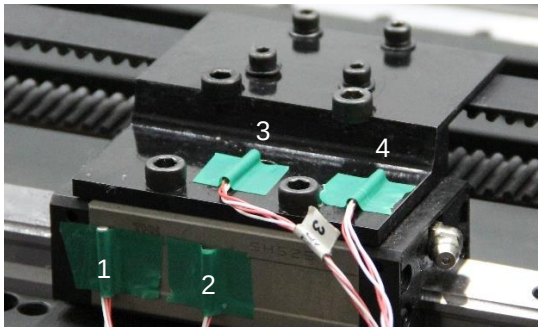

Fig. 5. *The locations of the four monitoring thermal sensors.*

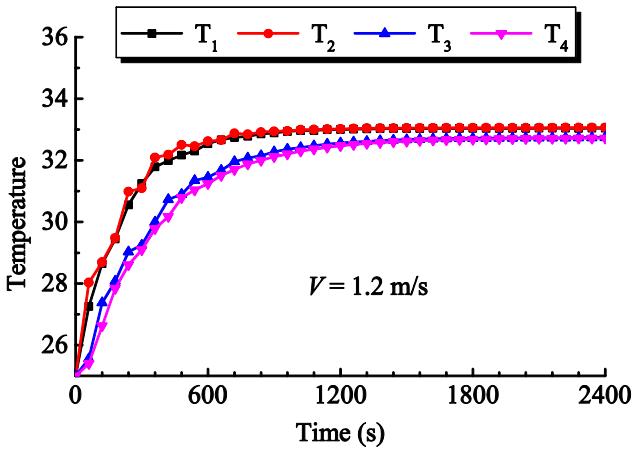

Fig. 6. *The measured temperature of the sliding carriage at monitoring locations.*

V. CONCLUSIONS

This paper presents a FE model combined with an analytical method to quantify the heat generation and transfer processes of the linear rolling guides during operation, which were validated by a simple linear guide system with NI temperature tests. The heat generated at the contact rolling interface considers the sliding friction, spinning friction and elastic hysteresis friction, and the FE model considers the convection effect of the structure. The numerical predicted surface temperatures of the carriage under different operating conditions show good agreements with experimental results, and the maximum percentage errs between them of the two sets data are within 3.24% and 3.17%, which indicates that the proposed FE model with the calculated analytical thermal parameters can

accurately predict the heat generation and transfer processes of the linear rolling guide during operation. Future work will focus on the temperature characteristic of the linear rolling guide under different lubrication conditions.

TABLE Ⅰ. TEMPERATURE OF THE CARRIAGE AT SPECIFIED LOCATIONS WITH DIFFERENT OPERATING CONDITIONS

Method		Temperature（℃）			
		T_1	T_2	T_3	T_4
Set 1	FEM	31.99	32.03	31.97	31.94
	Test	33.06	32.95	32.78	32.71
	Err	3.24%	2.79%	2.47%	2.35%
Set 2	FEM	35.76	35.86	35.72	35.68
	Test	36.93	37.02	36.78	36.65
	Err	3.17%	3.13%	2.88%	2.65%

ACKNOWLEDGMENT

This research was supported by the Natural Science Foundation of Guangdong Province of China (project nos. 508311819107) and Research Innovation Fund of Shenzhen City of China (project no. JCYJ20150805142729431).

REFERENCES

[1] J. Bryan, “International Status of Thermal Error Research,” CIRP Annals - Manufacturing Technology, vol. 39(2), pp. 645-656, 1990.

[2] J. Mayr, J. Jedrzejewski, E. Uhlmann, M. Alkan Donmez, W. Knapp, F. Härtig, et al., “Thermal issues in machine tools,” CIRP Annals-Manufacturing Technology, vol. 61, pp. 771-791, 2012.

[3] J. Xia, B. Wu, Y. Hu, T. Shi, “Experimental research on factors influencing thermal dynamics characteristics of feed system,” Precision Engineering, vol. 34(2), pp. 357-368, 2010.

[4] J. Takabi and M.M. Khonsari, “Experimental testing and thermal analysis of ball bearings,” Tribology International, vol. 60, pp. 93-103, 2013.

[5] C. Jin, B. Wu, and Y. Hu, “Heat generation modeling of ball bearing based on internal load distribution,” Tribology International, vol. 45(1), pp. 8-15, 2012.

[6] S.K. Kim and D.W. Cho, “Real-time estimation of temperature distribution in a ball-screw system,” International Journal of Machine Tools & Manufacture, vol. 37(4), pp. 451-464, 1997.

[7] C.H. Wu and Y.T. Kung, “Thermal analysis for the feed drive system of a CNC machine center,” International Journal of Machine Tools and Manufacture, vol. 43(15), pp. 1521-1528, 2003.

[8] Z. Z. Xu, X.J. Liu, H.K. Kim, J.H. Shin, S.K. Lyu, “Thermal error forecast and performance evaluation for an air-cooling ball screw system,” International Journal of Machine Tools & Manufacture, vol. 51(7), pp. 605-611, 2011.

[9] U. Heisel, G. Koscsák and T. Stehle, “Thermography-Based Investigation into Thermally Induced Positioning Errors of Feed Drives By Example of a Ball Screw,” CIRP Annals - Manufacturing Technology, vol. 55(1), pp. 423-426, 2006.

[10] S.C. Huang, “Analysis of a model to forecast thermal deformation of ball screw feed drive systems,” International Journal of Machine Tools and Manufacture, vol. 35(8), pp.1099-1104, 1995.

[11] S. Gleich, “Approach for Simulating Ball Bearing Screws in Thermal Finite Element Simulation,” Journal of Machine Engineering, vol. 7(1), pp. 101-107, 2007.

[12] Z. Winiarski, “Decreasing of Thermal Errors in a Lathe by Forced Cooling of Ball Screws and Headstock,” Journal of Machine Engineering, vol. 8(4), pp. 122-130, 2008.

[13] G. Szwengier, T. Goduński and S. Berczyński, “Identification of physical parameters in contact joints models of machines supporting systems,” Advances in Engineering Software, vol. 31(2), pp. 149-155, 2000.

[14] L. Kania, “Modelling of rollers in calculation of slewing bearing with the use of finite elements,” Mechanism and Machine Theory, vol. 41(11), pp. 1359-1376, 2006.

[15] T.A. Harris, M.N. Kotzalas, Rolling bearing analysis, 5th ed. NewYork: Taylor & Francis Group, 2006.

[16] F. Al-Bender, W. Symens, “Characterization of frictional hysteresis in ball- bearing guideways,” Wear, vol. 258, pp. 1630-1642, 2005.

[17] K. Kurpisz, A.J. Nowak, Inverse Thermal Problems. Southampton: Computational Mechanics Publications, 1995.

[18] S. Mostafa Ghiaasiaan, Convective Heat and Mass Transfer. New York: Cambridge University Press, 2011.